

EIGENMODES OF ISOSPECTRAL DRUMS*

TOBIN A. DRISCOLL[†]

Abstract. Recently it was proved that there exist nonisometric planar regions that have identical Laplace spectra. That is, one cannot “hear the shape of a drum.” The simplest isospectral regions known are bounded by polygons with reentrant corners. While the isospectrality can be proven mathematically, analytical techniques are unable to produce the eigenvalues themselves. Furthermore, standard numerical methods for computing the eigenvalues, such as adaptive finite elements, are highly inefficient. Physical experiments have been performed to measure the spectra, but the accuracy and flexibility of this method are limited. We describe an algorithm due to Descoux and Tolley [*Comput. Methods Appl. Mech. Engrg.*, 39 (1983), pp. 37–53] that blends singular finite elements with domain decomposition and show that, with a modification that doubles its accuracy, this algorithm can be used to compute efficiently the eigenvalues for polygonal regions. We present results accurate to 12 digits for the most famous pair of isospectral drums, as well as results for another pair.

Key words. eigenvalues, elliptic operators, isospectrality, finite-element methods, domain decomposition, method of particular solutions

AMS subject classifications. 65N25, 35P99, 35Q60

PII. S0036144595285069

1. Introduction. In 1966 Mark Kac [12] posed the question, “Can one hear the shape of a drum?” He was referring to the problem of whether the Laplacian operator with Dirichlet boundary conditions could have identical spectra on two distinct planar regions. Recently Gordon, Webb, and Wolpert [11] answered the question negatively via an elegantly constructed counterexample, justifiably attracting a great deal of attention [7, 8, 15]. The simplest form of their example is a pair of regions bounded by eight-sided polygons, henceforth called the GWW isospectral drums; see Figure 1.1. Numerous similar examples have since been discovered [5].

The simplest and most versatile proof of isospectrality employs “transplantation” [4] of the eigenfunctions. The regions are shown to be (or are constructed to be) made up of nonoverlapping translations, rotations, and reflections of a single shape, such as a triangle. Given an eigenfunction on one region, one can prescribe a function over the other region whose values over each piece are linear combinations of the eigenfunction values over several of the pieces of the first region. The combinations are chosen to satisfy the boundary conditions and to match values and derivatives at interfaces between pieces, and the interior equation is satisfied by superposition. Hence the result is an eigenfunction of the second region having the same eigenvalue. To complete the proof of isospectrality, one need only check that the procedure is invertible. Note that the proof is nonconstructive and other information, particularly the actual values of the eigenvalues, remains unknown.

To find the eigenvalues, it is natural to turn to numerical computation. However, straightforward numerical procedures for computing the eigenvalues [14] are inefficient because of the presence of reentrant corners. Even an adaptive approach, such as Bank’s PLTMG [3], obtains very slow convergence for the eigenvalue estimates.

*Received by the editors April 24, 1995; accepted for publication (in revised form) March 13, 1996. This work was supported by DOE grant DE-FG02-94ER25199.

<http://www.siam.org/journals/sirev/39-1/28506.html>

[†]Center for Applied Mathematics, Cornell University, Ithaca, NY 14853 (driscoll@na-net.ornl.gov).

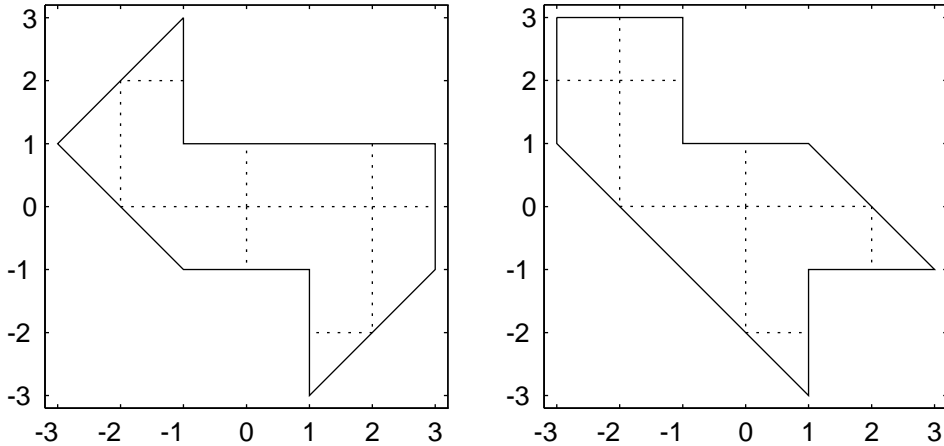


FIG. 1.1. *The GWW isospectral drums and subdivisions used for the domain decomposition method.*

Another well-known technique for eigenvalue problems, the method of particular solutions [10], fails to produce estimates of accuracy better than a few percent.

The first successful determination of the spectra of the GWW drums was by Sridhar and Kudrolli [16], who used an experimental approach. They constructed microwave cavities in the shapes of the polygons and measured resonances in transverse magnetic waves, which obey the Helmholtz equation. In this manner they obtained the first 54 eigenvalues to within about 0.3%. The accuracy and versatility of this method are limited primarily by the fabrication of the cavities.

More recently, Wu, Sprung, and Martorell [18] used a mode matching numerical approach to compute 25 eigenvalues of the GWW drums and compared their results to values extrapolated from finite difference calculations. Their mode matching approach is efficient, but it depends upon the region being decomposed into simple shapes for which all the eigenmodes can be explicitly written in closed form. We shall show that the figures computed by Wu et al. [18] are accurate to about four digits.

A little-known numerical method due to Descloux and Tolley [9] is intended specifically for eigenvalue computations on polygons. This algorithm, which is a combination of domain decomposition and singular finite-element methods, is applicable to any planar polygon and can efficiently compute eigenvalues to an accuracy on the order of the square root of machine precision. With a small modification, the accuracy of the method can be improved to the order of machine precision. Using this improved method, we have computed the first 25 eigenvalues of the GWW isospectral drums to an accuracy of at least 12 digits. Each eigenvalue calculation takes a few minutes on a workstation, and eigenfunctions can be computed just as quickly at arbitrary domain points.

In this paper we describe some of the limitations of the standard numerical approaches to computing the eigenvalues of the GWW drums. We then outline the domain decomposition method of Descloux and Tolley and describe our accuracy-doubling modification. We present numerical and graphical results of eigenvalue calculations for the GWW drums, comparing our results to the previously published estimates described above. A comparison is made of the method's efficiency with that of finite-element software packages. We also present the results of this method applied to another pair of polygonal isospectral drums.

2. Algorithms. Given a planar region Ω with polygonal boundary $\partial\Omega$, our goal is to find approximations to one or more eigenpairs $(\lambda, u) \in (\mathbf{R}^+, C(\overline{\Omega}))$ satisfying

$$(2.1a) \quad \Delta u + \lambda u = 0 \quad \text{in } \Omega,$$

$$(2.1b) \quad u = 0 \quad \text{on } \partial\Omega.$$

A direct numerical approach to this problem is to use a finite-element software package. We chose PLTMG [3] because of its widespread availability and automatic adaptive mesh refinement capabilities. PLTMG regards the linear problem (2.1) as a nonlinear continuation problem with parameter λ and functional $\rho(u) = \|u\|_{L^2}$. The procedure, which is outlined in section 4.6.2 of [3], is to track the zero solution for varying λ until a bifurcation point in the λ - ρ plane is found, at which point the bifurcating branch with constant λ (the eigenfunction) is followed. The grid is adaptively improved and the estimate for λ updated until the desired accuracy is apparently achieved.

Because the use of the nonlinear continuation method is atypical for the linear eigenvalue problem, we have additionally applied to this problem the PDE Toolbox for MATLAB, which also uses piecewise linear finite elements. Here the eigenvalue estimates come from the solution of a generalized matrix eigenproblem in the usual way. As with PLTMG, we adaptively refine the mesh based on a posteriori error estimates of the most recent solution.

An eigenfunction has a particular singular behavior at a corner of the boundary. If (u, λ) is an eigenpair and (r, ϕ) are suitably oriented polar coordinates originating from a corner of $\partial\Omega$ with interior angle π/α , then

$$(2.2) \quad u(r, \phi) = \sum_{n=1}^{\infty} c_n J_{n\alpha}(\sqrt{\lambda}r) \sin(n\alpha\phi),$$

where J_ν is a Bessel function of the first kind. This expression, which is essentially just a Fourier series, is valid at least for r less than the distance to the nearest other corner of $\partial\Omega$. At a reentrant corner, $\alpha < 1$ and the loss of smoothness in the solution causes an adaptive mesh to be highly refined at the corner. The direct use of this expansion leads to much more efficient algorithms for the problem (2.1).

One approach to exploiting this information is the method of particular solutions, or point matching [14], introduced by Fox, Henrici, and Moler [10], who illustrated its use with an L-shaped region.¹ This method truncates the expansion (2.2) taken about the reentrant corner(s) and determines eigenvalues by requiring the trial solution to be zero at collocation points along the boundary $\partial\Omega$. In practice, this reduces to detecting singularity in a matrix which depends nonlinearly on a parameter λ . However, as the authors note, this method does not work well for regions with more than one reentrant corner, and our experience bears this out. The difficulty is that as the number of terms in the truncated expansion is increased, the matrix becomes very nearly singular for all values of λ , and detecting the true singularity numerically becomes impossible. In fact, we have been unable to produce more than two or three accurate digits for a few of the smallest eigenvalues with this method, even after including expansions about all of the corners.

It seems more appropriate to treat the eigenfunction expansions in (2.2) locally rather than globally. To this end, let the polygon Ω be subdivided into several nonoverlapping pieces Ω_j , $j = 1, \dots, N$. We denote each interface $\partial\Omega_j \cap \partial\Omega_k$, which may be

¹Their calculations are the basis of the logo of The MathWorks, Inc. and can be demonstrated with the `membrane` command in MATLAB.

empty, by Γ_{jk} . Suppose that, given a scalar λ , we can find a set of N “subfunctions” $u_j \in C(\overline{\Omega_j})$ such that (λ, u_j) is a certain eigenpair on subregion Ω_j :

$$(2.3a) \quad \Delta u_j + \lambda u_j = 0 \quad \text{in } \Omega_j,$$

$$(2.3b) \quad u_j = 0 \quad \text{on } \partial\Omega \cap \partial\Omega_j.$$

(Note the difference between boundary conditions (2.1b) and (2.3b).) It is well known that λ is an eigenvalue for the whole region Ω if and only if along each nonempty interface Γ_{jk} , the subfunctions u_j and u_k and their normal derivatives match continuously. This fact is at the root of the transplantation proof of isospectrality, and an analogous observation underlies many domain decomposition methods from the numerical solution of elliptic PDEs [6].

The method of mode matching described by Wu, Sprung, and Martorell [18] is one way to exploit this idea. In this method, the expansion (2.2) is not used. Instead, analytic expressions of the solutions to (2.3) must be known throughout each subdomain Ω_j . For the GWW drums of Figure 1.1, it is possible to accomplish this by dividing each drum into five pieces, each of which is a square or a $(45^\circ, 45^\circ, 90^\circ)$ triangle. Because of the simple shapes, the eigenfunctions are differences between products of sine functions. A subfunction u_j is expanded as a combination of these functions with unknown coefficients, the expansions are truncated, and the requirement of functions and derivatives matching at interfaces becomes a linear system in these coefficients. As with the method of particular solutions, an eigenvalue is a value of λ for which the matrix of this system becomes singular. In this case, however, Wu et al. report no difficulty with numerical near-singularity.

A shortcoming of the mode matching method is that it is not universally applicable. In general, we cannot expect Ω to admit a simple decomposition for which the eigenfunctions of the individual pieces can be explicitly written in a convenient and usable form. A universal algorithm ought to return to the expansion (2.2), which is always available.

Now let us assume that the boundary of each Ω_j includes a portion of the boundary of the whole region Ω in such a way that exactly one vertex V_j with interior angle θ_j of the original polygon is in $\partial\Omega_j$. Let $r_j = \max_{z \in \Omega_j} |z - V_j|$ and $\rho_j = \min_{k \neq j} |V_k - V_j|$. To guarantee convergence, we require that $r_j < \rho_j$. We may add extra vertices to $\partial\Omega$ with $\theta_j = \pi$. (Some polygons, such as a regular hexagon, require one or more interior elements to meet this condition, but this is easily accommodated; see [9].) In Figure 1.1 we illustrate one such subdivision for the GWW isospectral polygons.

We could now enforce the matching conditions at collocation points on the interfaces, in the manner of the method of particular solutions. However, Descloux and Tolley [9] again find the problem with numerical singularity of the resulting matrix and instead propose a method that employs finite-element ideas within the domain decomposition framework. At the heart of their algorithm are the functionals

$$(2.4) \quad R(\lambda; u_1, \dots, u_N) = \sum_{j < k} \int_{\Gamma_{jk}} [(u_j - u_k)^2 + |\nabla u_j - \nabla u_k|^2] ds,$$

$$(2.5) \quad M(\lambda; u_1, \dots, u_N) = \sum_{j=1}^N \iint_{\Omega_j} u_j^2 dx dy.$$

For fixed λ , let $\mu(\lambda)$ be the minimum of the quotient R/M over all choices of sub-

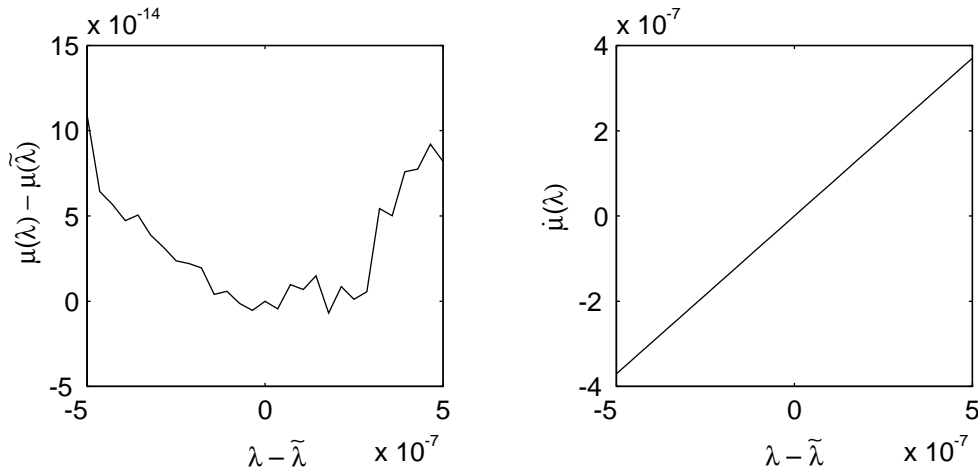


FIG. 2.1. Comparison of $\mu(\lambda)$ with $\dot{\mu}(\lambda)$ near a minimum $\tilde{\lambda}$, which is an estimate of the first GWW eigenvalue.

functions. Now $\mu(\lambda) = 0$ if and only if λ is an eigenvalue of (2.1) and each u_j is the restriction of the eigenfunction u to Ω_j .²

We now use the finite-element idea of replacing a minimization over infinite-dimensional function spaces by minimization over a nested family of finite-dimensional approximations. As bases for these spaces we choose terms of the local Fourier–Bessel expansions; that is, each subfunction u_j is expressed as a combination of n_j terms of the expansion (2.2) about V_j . This guarantees that the subproblem (2.3) is satisfied, even when λ is not an eigenvalue of Ω .³ For optimal performance, n_j should be proportional to θ_j , the interior angle at V_j .

The corresponding approximation to $\mu(\lambda)$ now becomes the solution to a generalized matrix eigenproblem:

$$(2.6) \quad A(\lambda)v(\lambda) = \mu(\lambda)B(\lambda)v(\lambda).$$

The matrix A is computed by evaluating (2.4) by Gauss–Legendre quadrature with q nodes on each interface, and (2.5) is approximated by integrals over circular sectors so as to make the mass matrix B diagonal. This diagonality makes it convenient to replace the generalized eigensystem by the standard eigenproblem for $B^{-1/2}AB^{-1/2}$. Finally, a value of λ which minimizes our approximation to μ is taken as an estimate of an eigenvalue of (2.1a)–(2.1b).

Here is where we improve upon Descloux and Tolley’s original algorithm. Suppose we can compute μ only to accuracy ϵ , which is on the order of machine precision. Because of the quadratic nature of μ near a minimum, a straightforward minimization gives an accuracy in λ of only order $\sqrt{\epsilon}$. If instead we seek solutions to $\dot{\mu}(\lambda) = 0$, the linearity of $\dot{\mu}$ near a minimum allows us to find λ to an accuracy comparable to that of μ . Figure 2.1 illustrates the situation for an estimate $\tilde{\lambda}$ of the first eigenvalue

²Descloux and Tolley were able to prove convergence of their algorithm only when gradients, rather than normal derivatives, appear in (2.4).

³Actually, $\partial\Omega \cap \partial\Omega_j$ may contain isolated points where the boundary condition (2.3b) is not explicitly satisfied. However, the matching conditions do enforce this condition, and experiments show that slight changes in the Ω_j that avoid this problem do not substantially affect the performance of the algorithm.

TABLE 3.1

The first 25 eigenvalues of the GWW isospectral drums. All digits shown are believed to be correct.

2.53794399980	9.20929499840	14.3138624643	20.8823950433	24.6740110027
3.65550971352	10.5969856913	15.8713026200	21.2480051774	26.0802400997
5.17555935622	11.5413953956	16.9417516880	22.2328517930	27.3040189211
6.53755744376	12.3370055014	17.6651184368	23.7112974848	28.1751285815
7.24807786256	13.0536540557	18.9810673877	24.4792340693	29.5697729132

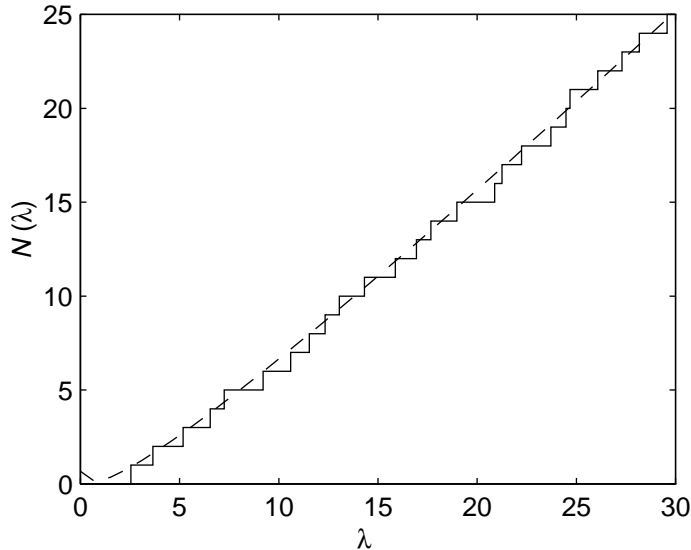


FIG. 3.1. Integrated eigenvalue density for the GWW drums. The solid staircase is the actual density, compared with the dashed line representing Weyl's formula (3.1).

of the GWW drums. By differentiating (2.6) with respect to λ and left-multiplying through by v^T , we see that

$$(2.7) \quad \dot{\mu}(\lambda) = \frac{v^T(\dot{A} - \mu\dot{B})v}{v^T B v}.$$

The matrices \dot{A} and \dot{B} can be computed in a straightforward manner.

To summarize, the algorithm can be viewed as an iteration in the parameter λ whose convergence is dictated by domain decomposition considerations. Each step of the iteration is computed approximately by a large singular finite-element method, where the basis functions depend nonlinearly on the parameter λ . Improved accuracy is achieved by increasing the number of basis functions in the inner step, as with p -type finite-element methods.

3. Results. In Table 3.1 we list our estimates of the first 25 eigenvalues of the GWW isospectral drums. For these calculations we used $n_j = 36/\alpha_j = 36\theta_j/\pi$ basis functions in region Ω_j and $q = 40$ Gauss quadrature points on each interfacial line segment. The results for the two drums agree with each other nearly to machine precision.

In Figure 3.1 we compare $N(\lambda)$, the number of eigenvalues (counting multiplicity) less than λ , to the corrected Weyl formula, which for a polygon is [2]

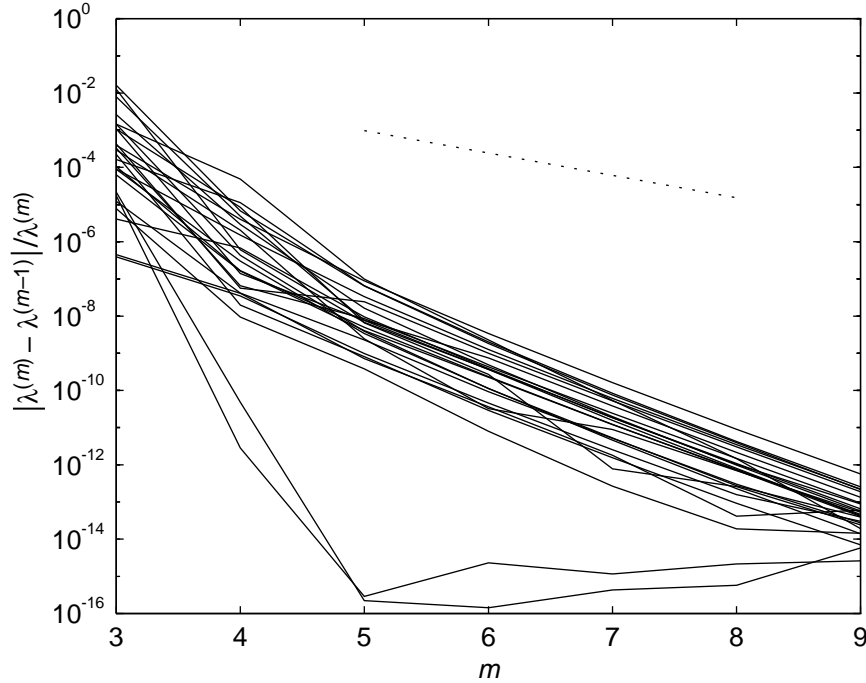


FIG. 3.2. *Convergence of the eigenvalue estimates. The dotted line shows the theoretically worst-case convergence ω^m , with ω given by (3.2). See the text for comments about the two dramatically decreasing curves.*

$$(3.1) \quad N(\lambda) \approx \frac{A}{4\pi} \lambda - \frac{P}{4\pi} \sqrt{\lambda} + \sum_{j=1}^N \frac{1}{24} (\alpha_j - \alpha_j^{-1}),$$

where A is the area of the region Ω and P is its perimeter. (By isospectrality, A and P are necessarily the same for the two drums.) The formula agrees excellently with the exact $N(\lambda)$.

We believe that the entries of Table 3.1 are accurate to all digits shown. As support for this claim, in Figure 3.2 we present the convergence history of the estimates with respect to $n_j = 4m/\alpha_j$. For each value of m , we find that the estimates of any eigenvalue for the two drums agree essentially to machine precision, and we use $\lambda^{(m)}$ to denote this common number. Figure 3.2 shows the relative change in the successive estimates $\lambda^{(m)}$ as m varies. Descloux and Tolley prove geometric convergence of their algorithm and identify a lower bound on the rate:

$$(3.2) \quad \omega = \max_j \left[\left(\frac{r_j}{\rho_j} \right)^{n_j \alpha_j / m} \right] = \max_j \left[\left(\frac{\max_{z \in \Omega_j} |z - V_j|}{\min_{k \neq j} |V_k - V_j|} \right)^{n_j \alpha_j / m} \right].$$

Here, $\omega = 1/4$. However, the observed rate of convergence is much better, about ω^2 . In general, curves which are higher on the graph correspond to higher eigenvalues, the two “superconvergent” curves being exceptions which are discussed below. Note that all the convergence curves end at less than 10^{-12} .

As mentioned previously, a feature of the results is the dramatic agreement for all the estimates of the two drums, regardless of their accuracy. In fact, all the

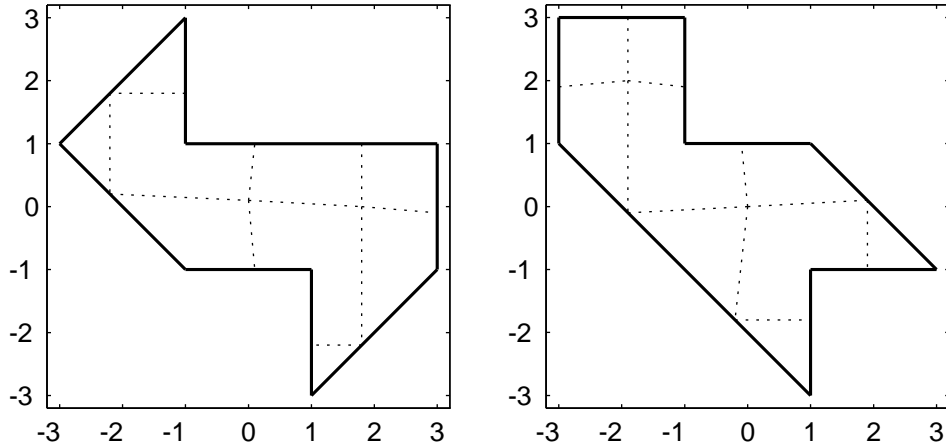
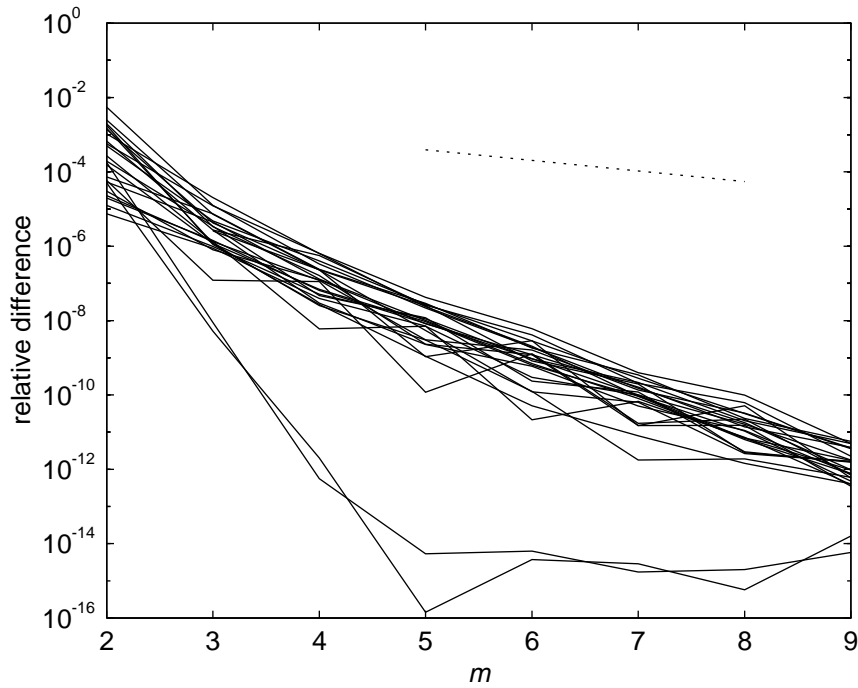


FIG. 3.3. An alternate subdivision of the GWW drums.

FIG. 3.4. Difference in estimates for the two drums at each m when using the subdivisions of Figure 3.3.

eigenvalues of the generalized system (2.6), and hence $\mu(\lambda)$, are numerically identical for the two regions for any m . Presumably this occurs because the subdivisions of Figure 1.1 respect the transplation symmetries between the regions. To further check our results, we applied the algorithm using the less regular subdivisions, selected arbitrarily, depicted in Figure 3.3. The estimates for the two regions now differ by amounts consistent with their apparent accuracy. In Figure 3.4 we compare the differences between estimates for the two drums to the predicted convergence ω^m ,

where for this subdivision $\omega \approx 0.52$. Again, the observed convergence is about twice as fast. The estimates for $m = 11$ all agree with the numbers of Table 3.1 to the full 12 digits.

Figures 3.5 and 3.6 show in detail the first eight eigenfunctions of the GWW drums, including the nodal lines. For comparison, in Figure 3.7 we reproduce the results of microwave measurements made by Sridhar and Kudrolli [16] for modes 1, 3, and 6. The microwave results, while noisy, do recognizably represent the shapes of the modes.

Figure 3.8 shows contours for the ninth mode, which is clearly equivalent to the first mode on a $(45^\circ, 45^\circ, 90^\circ)$ triangle. This triangle is the fundamental shape that forms the basis of the transplantation proof. The exact eigenvalue in this case is $5\pi^2/4$, which agrees with our computed values to 15 digits. A similar phenomenon occurs at the 21st mode, which is equivalent to the second mode on the triangle with eigenvalue $10\pi^2/4$. In fact, these two modes account for the “superconvergent” curves of Figures 3.2 and 3.4. We hypothesize that the accelerated convergence occurs because the symmetries of these eigenfunctions about the corners cause many of the Fourier coefficients in (2.2) to be exactly zero.

In Figure 3.9 we compare our results to other published determinations of the first 25 eigenvalues. Based on their microwave experiments, Sridhar and Kudrolli report these eigenvalues to an rms relative accuracy of about 0.3%. We observe that the error in their estimates is frequently much larger than the agreement between their values, but there is no clear explanation for this phenomenon [13]. The eigenvalues obtained by Wu, Sprung, and Martorell [18] by an extrapolation of results from finite differences and mode matching agree with our results to about three and four digits, respectively.⁴

In Figure 3.10 we compare the efficiency of the domain decomposition method to the computation of the eigenvalues in PLTMG and the PDE Toolbox for MATLAB. Figure 3.11 shows the adaptive grid process in PLTMG for the first eigenvalue on the first drum. The finest structure occurs near the corner where the eigenfunction is large. At this stage, there are 966 triangles and 402 vertices, and the eigenvalue estimate is about 2.5659. If one were to try to obtain 12 digits via either of the finite-element methods, storage as well as computational time would become a serious obstacle.

One advantage of the domain decomposition method over physical experiment and mode matching is its flexibility in application to other polygons. We have applied the domain decomposition method to another pair of isospectral drums, depicted in Figure 3.12. These regions were constructed using the techniques of Buser et al. [5]. The fundamental unit of the construction is a $(30^\circ, 70^\circ, 80^\circ)$ triangle, which renders the mode matching method impractical. The first 10 eigenvalues of these regions are listed in Table 3.2 to nine digits. In Figure 3.13 we present the convergence history analogous to Figure 3.2. The convergence is again much faster than the minimum rate of $\omega \approx 0.48$. Selected eigenfunctions for these drums are displayed in Figure 3.14.

4. Conclusions. Elliptic problems on regions with corners, especially reentrant corners, are recognized as numerically difficult. Indeed, general-purpose packages such as PLTMG do not use known information about the singularities of solutions near the corners, and the method of particular solutions uses this information only globally, restricting its usefulness. There is a mode matching method that exploits certain special geometries, but this method does not apply to arbitrary polygons.

⁴In the mode matching method, the degenerate modes 9 and 21 are not computed but are taken exact.

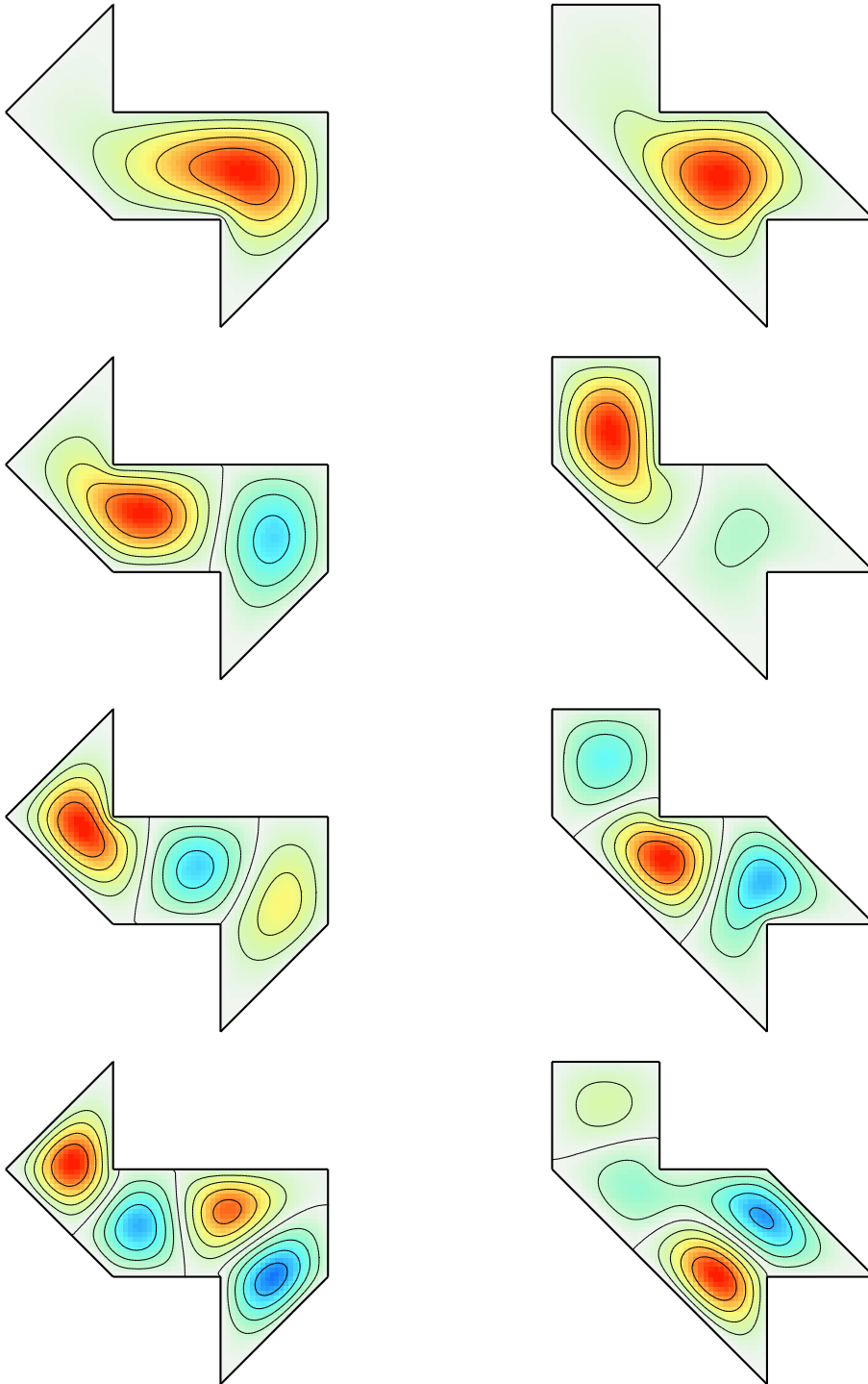


FIG. 3.5. First four eigenfunctions of the GW isospectral drums. Each is normalized to have unit amplitude. The contours are at levels $-0.8, -0.6, \dots, 0.8$.

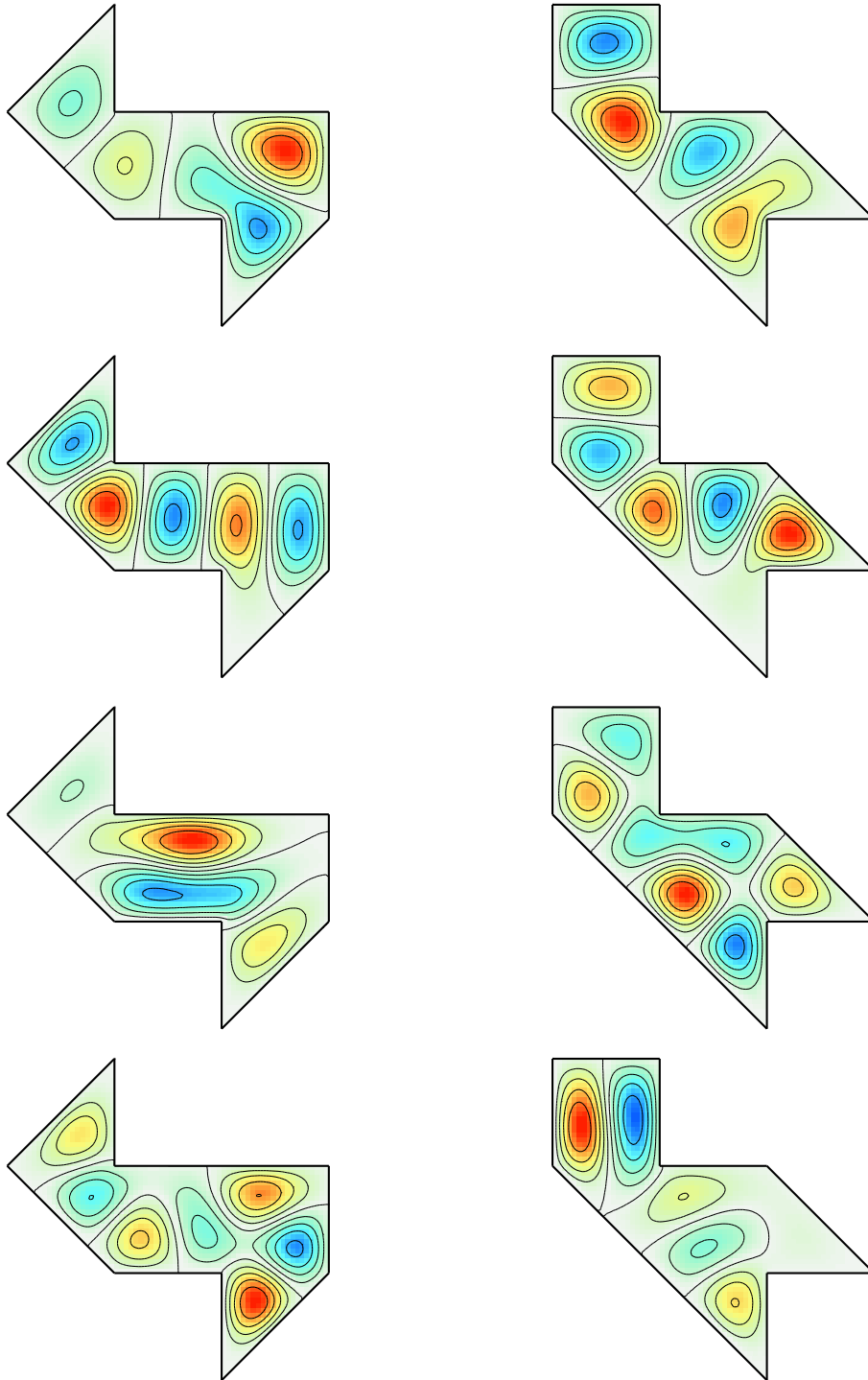


FIG. 3.6. *Eigenfunctions 5–8 of the GWW isospectral drums.*

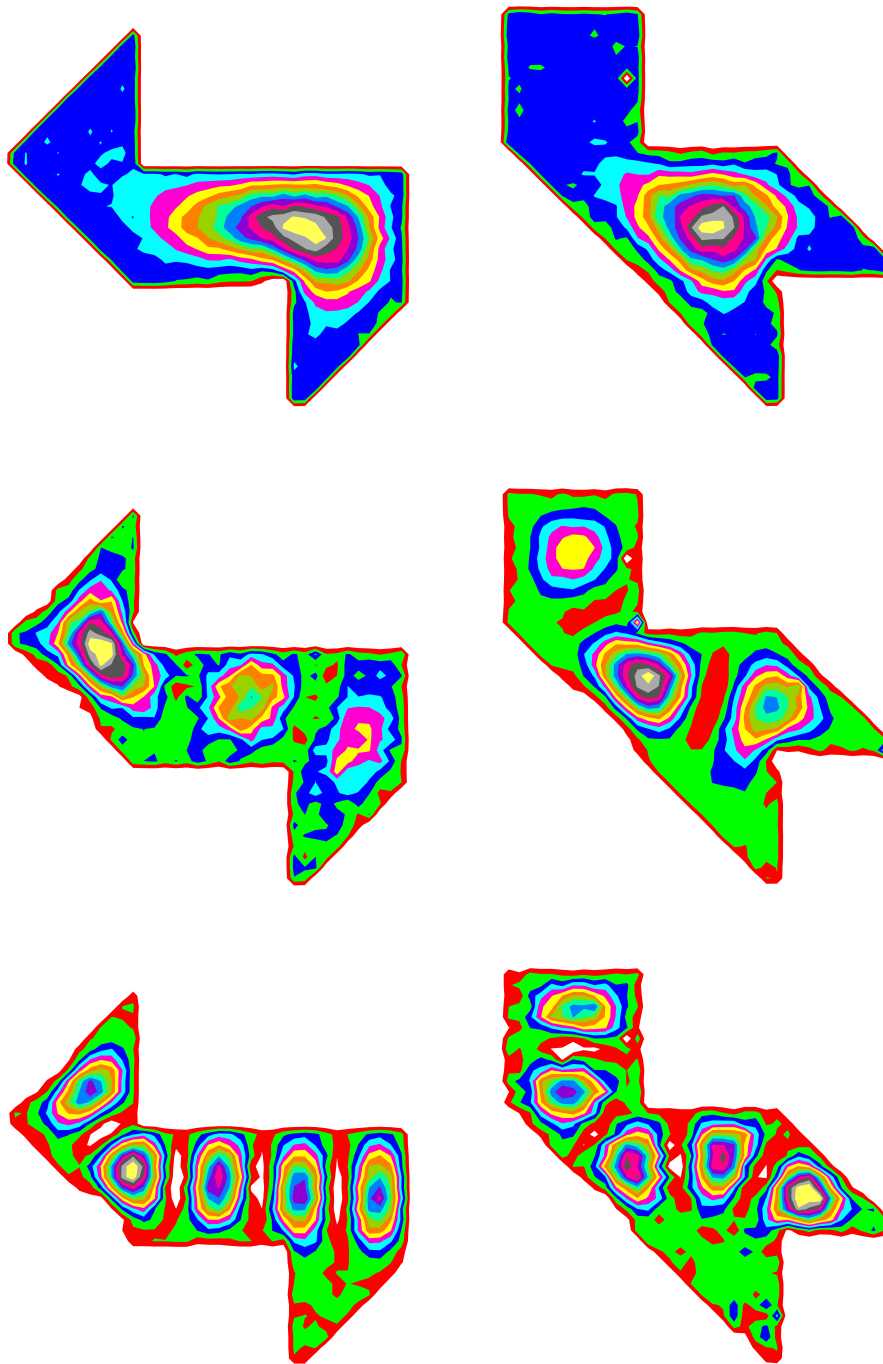


FIG. 3.7. *Eigenfunctions 1, 3, and 6 of the GWW isospectral drums, as measured by Sridhar and Kudrolli in their microwave experiments. Reprinted with permission from S. Sridhar and A. Kudrolli.*

The domain decomposition method described above exploits the corner information in an appropriately local and completely general fashion. The method has exponential convergence as the size of the approximation basis increases. Using this algorithm, we have made the first high-precision determinations of the eigenvalues of

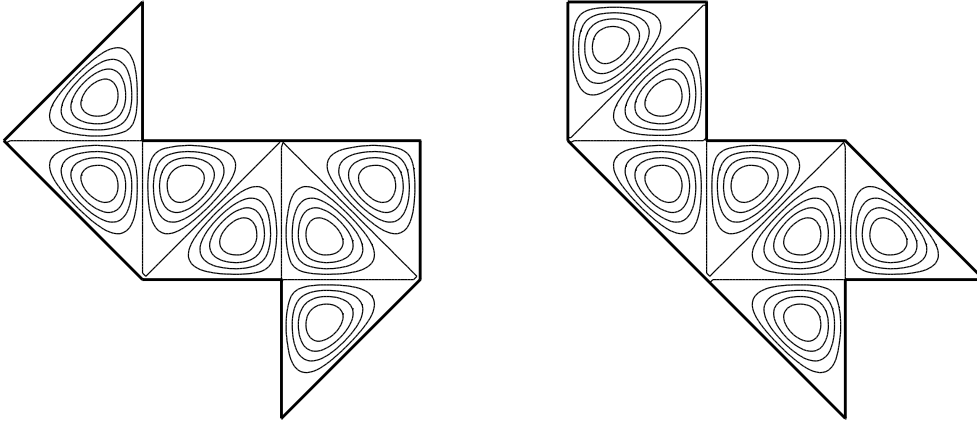


FIG. 3.8. *The ninth mode of the GWW drums. This corresponds to the first mode on a $(45^\circ, 45^\circ, 90^\circ)$ triangle.*

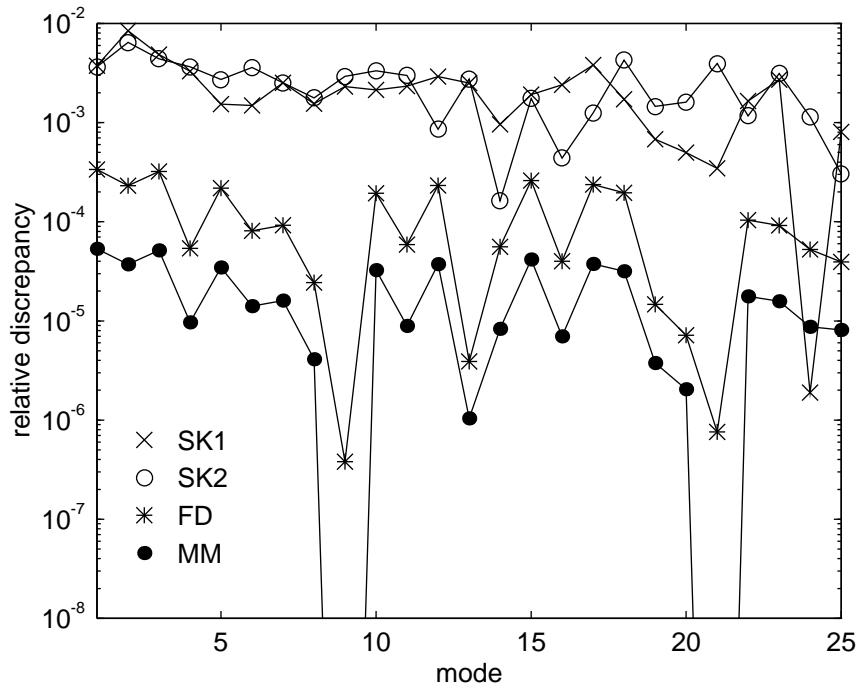


FIG. 3.9. *Comparison of our results with other determinations of the spectra. Shown are the two sets obtained by Sridhar and Kudrolli by microwave experiments and the results of finite differences and mode matching reported by Wu et al.*

the GWW drums. We have also demonstrated that the method is flexible enough to be applied to other instances of polygonal isospectral regions.

We do not claim that the algorithm presented here is the only efficient method possible for the polygon eigenvalue problem. For example, we have not explored the application of h - p finite-element methods [1] or integral equation techniques [17]. We do believe, however, that any competitive method will make explicit use of the solutions' behavior at the corners.

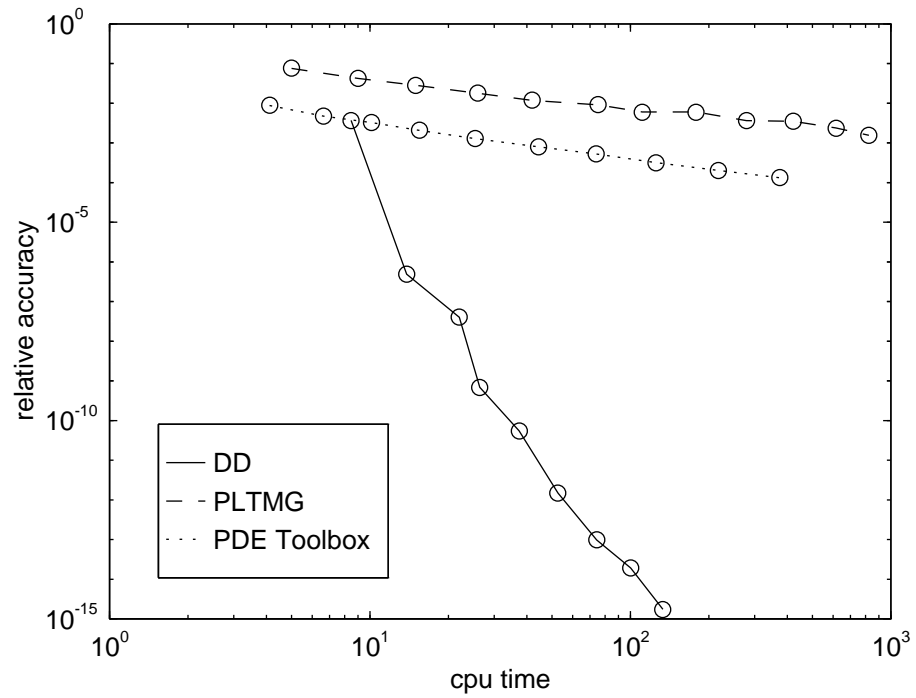


FIG. 3.10. Comparison of PLTMG with the domain decomposition method. The data are based on the computation of the first eigenvalue of the first GWW drum on a Sun SPARCstation 2.

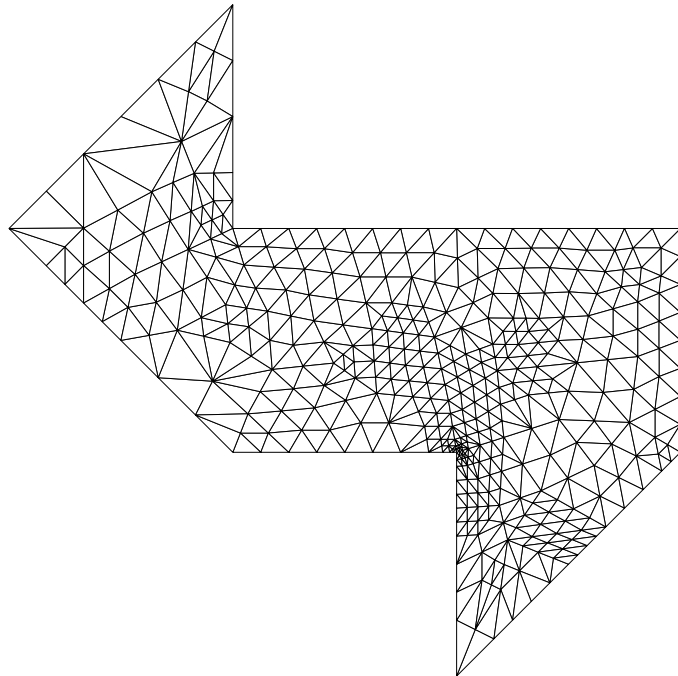


FIG. 3.11. Adaptive mesh refinement by PLTMG. The mesh is most refined near one of the reentrant corners.

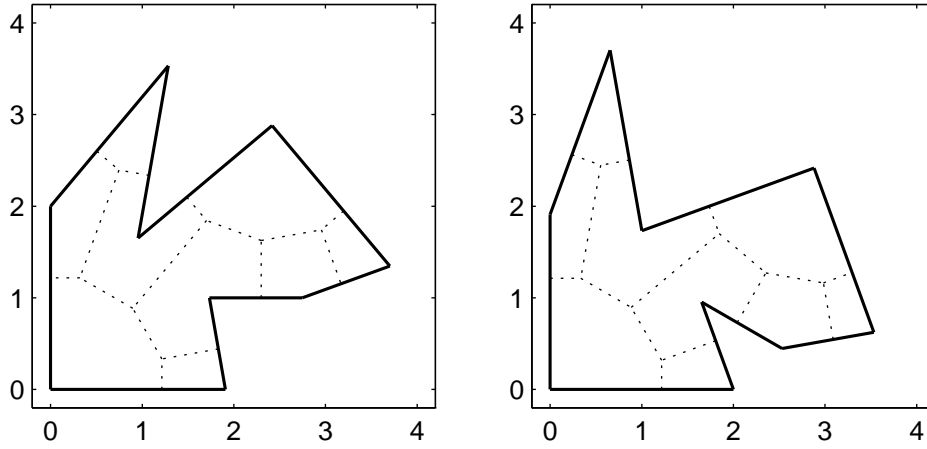


FIG. 3.12. Two more isospectral regions and the subdivisions used in the domain decomposition method.

TABLE 3.2
First 10 eigenvalues of the isospectral drums of Figure 3.12.

5.63126379	18.8537757
7.18148848	19.8509471
12.7905748	24.1803291
13.0935554	27.5379471
17.0680091	30.0098327

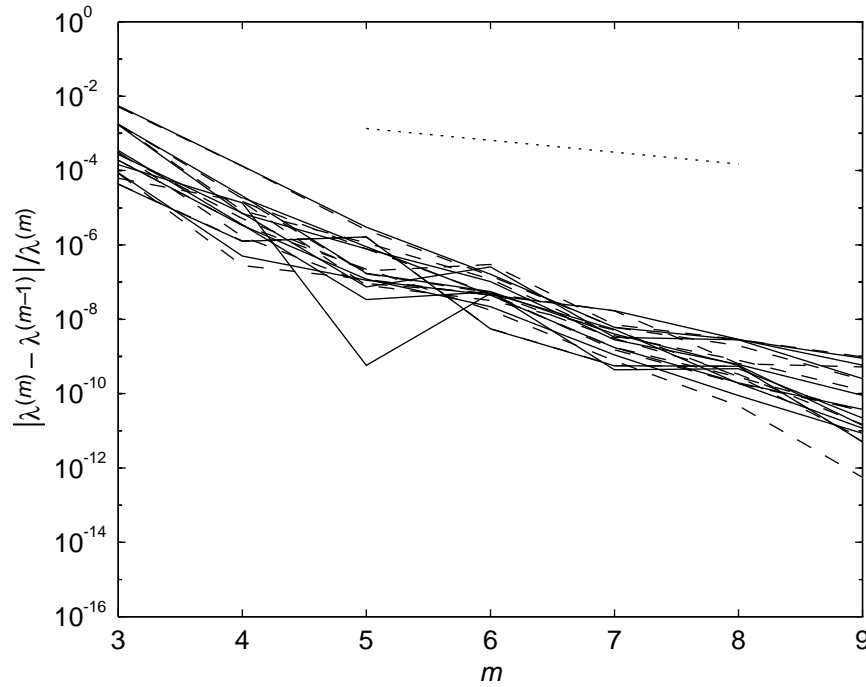


FIG. 3.13. Convergence of the eigenvalue estimates for the second pair of drums. Solid lines are for the first drum, dashed lines are for the second drum, and the dotted line is a multiple of ω^m , where $\omega \approx 0.48$.

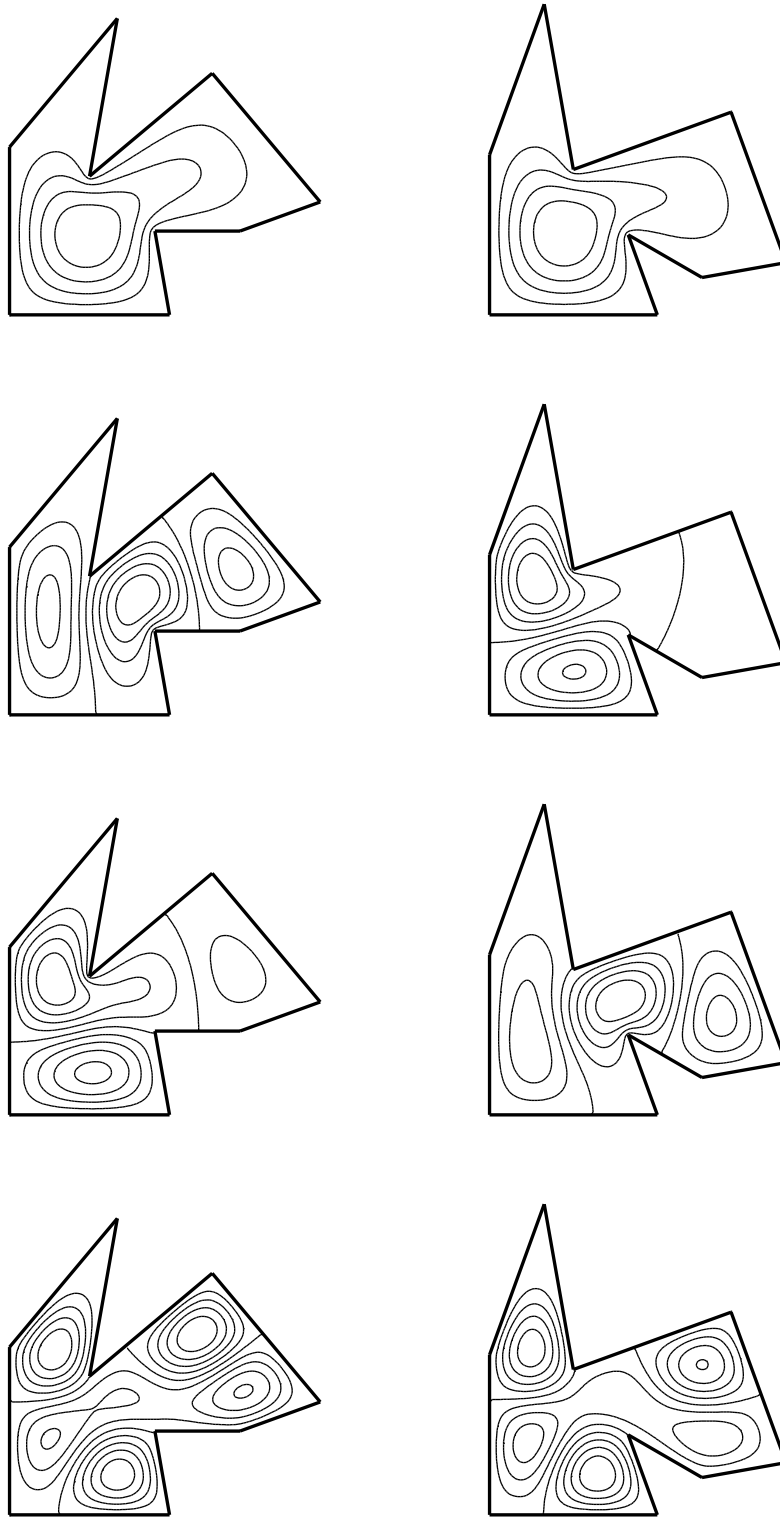


FIG. 3.14. *Eigenmodes 1, 3, 4, and 6 of the second pair of isospectral drums. Modes have unit amplitude and contours are drawn at $-0.8, -0.6, \dots, 0.8$.*

To see more of the eigenfunctions of the GWW drums and some animations of vibrations arising from selected combinations of the modes, use a WWW browser to open the URL <http://amath.colorado.edu/appm/faculty/tad>.

Acknowledgments. I would like to thank David Webb, Peter Doyle, Jean Descloux, S. Sridhar, and Arshad Kudrolli for their cooperation and pointers to relevant literature. I am also grateful to Steve Vavasis and Nick Trefethen for their valuable comments and suggestions.

REFERENCES

- [1] I. BABUŠKA AND M. SURI, *The P and H-P versions of the finite element method, basic principles and properties*, SIAM Rev., 36 (1994), pp. 578–632.
- [2] H. P. BALTES AND E. R. HILF, *Spectra of Finite Systems*, Bibliographisches Institut, Mannheim, 1976.
- [3] R. BANK, *PLTMG Users' Guide 7.0: A Software Package for Solving Elliptic Partial Differential Equations*, SIAM, Philadelphia, PA, 1994.
- [4] P. BÉRARD, *Transplantation et isospectralité*, Math. Ann., 292 (1992), pp. 547–559.
- [5] P. BUSER, J. CONWAY, P. DOYLE, AND K. SEMMLER, *Some planar isospectral domains*, Internat. Math. Res. Notices, (1994), pp. 391–400.
- [6] T. F. CHAN AND T. P. MATHEW, *Domain decomposition algorithms*, Acta Numerica, (1994), pp. 61–143.
- [7] S. J. CHAPMAN, *Drums that sound the same*, Amer. Math. Monthly, 102 (1995), pp. 124–138.
- [8] B. CIPRA, *You can't hear the shape of a drum*, Science, 255 (1992), pp. 1642–1643.
- [9] J. DESCLOUX AND M. TOLLEY, *An accurate algorithm for computing the eigenvalues of a polygonal membrane*, Comput. Methods Appl. Mech. Engrg., 39 (1983), pp. 37–53.
- [10] L. FOX, P. HENRICI, AND C. MOLER, *Approximations and bounds for eigenvalues of elliptic operators*, SIAM J. Numer. Anal., 4 (1967), pp. 89–102.
- [11] C. GORDON, D. WEBB, AND S. WOLPERT, *Isospectral plane domains and surfaces via Riemannian orbifolds*, Invent. Math., 110 (1992), pp. 1–22.
- [12] M. KAC, *Can one hear the shape of a drum?*, Amer. Math. Monthly, 73 part II (1966), pp. 1–23.
- [13] A. KUDROLLI, private communication, 1995.
- [14] J. R. KUTTLER AND V. G. SIGILLITO, *Eigenvalues of the Laplacian in two dimensions*, SIAM Rev., 26 (1984), pp. 163–193.
- [15] I. PETERSON, *Beating a fractal drum: How a drum's shape affects its sound*, Sci. News, 146 (1994), pp. 184–185.
- [16] S. SRIDHAR AND A. KUDROLLI, *Experiments on not "hearing the shape" of drums*, Phys. Rev. Lett., 72 (1994), pp. 2175–2178.
- [17] P. M. SWARZTRAUBER, *On the numerical solution of the dirichlet problem on a region of general shape*, SIAM J. Numer. Anal., 9 (1973), pp. 300–306.
- [18] H. WU, D. W. L. SPRUNG, AND J. MARTORELL, *Numerical investigation of isospectral cavities built from triangles*, Phys. Rev. E, 51 (1995), pp. 703–708.